Proceedings of the
47th IEEE Conference on Decision and Control
Cancun, Mexico, Dec. 9-11, 2008

How Springs Can Help to Stabilize Motions of Underactuated Systems with Weak Actuators

Uwe Mettin, Pedro X. La Hera, Leonid B. Freidovich, Anton S. Shiriaev

Abstract— **In the field of robotics the energy spent for actuation is always an issue. It is often the case that some desired motions cannot be achieved by the robot due to limitations in actuation power. We suggest a simple solution to the problem: complement the actuators by some configuration of mechanical springs which delivers a torque profile that is well-tuned for the desired robot motion. As a result, the control effort for the original actuator will be reduced. In this case study we consider an underactuated planar two-link robot for experimental demonstration of the concept. The virtual holonomic constraints approach serves as analytical tool to parameterize, plan, and stabilize desired periodic motions.**

Index Terms— **Motion Planning, Virtual Holonomic Constraints, Springs, Underactuated Mechanical Systems**

I. Introduction

Motion planning and feedback controller design are key issues in robotics. The application area of todays robots is broad: it covers manipulation tasks for standard robot arms, legged locomotion of mechanically sophisticated machines, robotic prosthetics and exoskeletons, etc. Naturally, the achievable performance of feedback controlled robots depends to a large extent on the power of available actuators. However, the actuators are normally chosen according to constraints in the construction, such as limited space, minimal mass, and power consumption. It means that many motions planned analytically based on appropriate models and confirmed throughout simulations might not be realizable in experiments. There are always some desired motions that require actuation power which is hardly feasible for the robot. That is why we are interested to answer the following question. Is it possible to improve the actuation range by introducing some passive mechanical elements in parallel to the original actuator?

Springs are simple mechanical devices that offer great functionality at low cost. They are commonly applied in machines to exert force, to provide flexibility, and to store or absorb energy [4]. Therefore, springs are particularly attractive to be used as complementary source of torque. The main task is to design a spring configuration that gives a torque profile somewhat close to the one that is required for a particular motion. As a result, the original actuator is mainly stabilizing this motion while the springs generate most of the nominal torque required.

This paper shows how to take advantage of mechanical springs to complement a comparably weak DC motor. The aim is to generate periodic motions of an underactutated planar two-link robot, the so-called Pendubot. Motion planning and control design of underactuated systems is clearly more challenging compared to the case when all degrees of freedom are actuated. Here, the main objective is to reduce the control efforts by augmenting the actuation with contributive spring torques. The Pendubot and the installed spring assembly are depicted in Fig. 1. Corresponding system dynamics as well as properties of the spring assembly are presented in Section II and Section III.

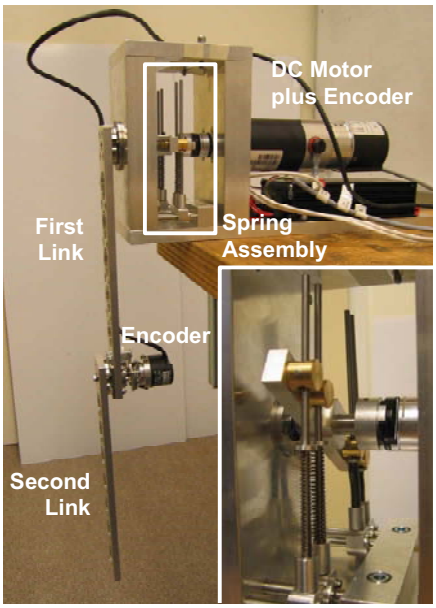

Fig. 1. Pendubot with spring assembly from Umeå University. The robot was designed and built by A. Sandberg and S. Elmå.

The *virtual holonomic constraints approach*, recently developed in [6], is used in Section IV and Section V as analytical tool to parameterize, plan, and stabilize desired periodic motions for the Pendubot. The underlying theory has been already applied in [1]. However, in this paper the focus lies on the contribution of springs complementary to the actuator which plays a role in the motion planning as well as in the feedback control action. Experimental results for a particular periodic motion are finally shown in Section VI and conclusions are drawn in Section VII.

U. Mettin, P. La Hera and L. Freidovich are with the Department of Applied Physics and Electronics, Umeå University, SE-901 87 Umeå, Sweden. E-mail: Uwe.Mettin@tfe.umu.se and {Xavier.LaHera|Leonid.Freidovich}@tfe.umu.se.

A. Shiriaev is with the Department of Applied Physics and Electronics, Umeå University, SE-901 87 Umeå, and the Department of Engineering Cybernetics, Norwegian University of Science and Technology, NO-7491 Trondheim, Norway. E-mail: Anton.Shiriaev@tfe.umu.se.

This work has been partly supported by the Kempe Foundation and the Swedish Research Council (under the grant 2005-4182).

II. Pendubot Dynamics

The dynamics of the planar two-link manipulating robot with actuation only on first link q_1 and a non-actuated link q_2 is given by [8]

$$M(q)\begin{bmatrix}\ddot{q}_1\\ \ddot{q}_2\end{bmatrix}+C(q,\dot{q})\begin{bmatrix}\dot{q}_1\\ \dot{q}_2\end{bmatrix}+G(q)=\begin{bmatrix}\tau\\ 0\end{bmatrix} \quad (1)$$

with the inertia matrix

$$M(q)=\begin{bmatrix}p_1+p_2+2p_3\cos(q_2) & p_2+p_3\cos(q_2)\\ p_2+p_3\cos(q_2) & p_2\end{bmatrix},$$

the matrix corresponding to Coriolis and centrifugal forces

$$C(q,\dot{q})=\begin{bmatrix}-p_3\sin(q_2)\dot{q}_2 & -p_3\sin(q_2)(\dot{q}_1+\dot{q}_2)\\ p_3\sin(q_2)\dot{q}_1 & 0\end{bmatrix},$$

and the gravitational torque vector

$$G(q)=\begin{bmatrix}p_4\cos(q_1)+p_5\cos(q_1+q_2)\\ p_5\cos(q_1+q_2)\end{bmatrix}.$$

The physical model parameters, given in Table I, are combined to

$$\begin{aligned}p_1&=m_1r_1^2+m_2l_1^2+J_{c1}=0.0319\,\mathrm{kg\,m^2}\\ p_2&=m_2r_2^2+J_{c2}=0.0092\,\mathrm{kg\,m^2}\\ p_3&=m_2l_1r_2=0.01\,\mathrm{kg\,m^2}\\ p_4&=(m_1r_1+m_2l_1)g=1.2954\,\mathrm{Nm}\\ p_5&=m_2r_2g=0.3915\,\mathrm{Nm}.\end{aligned}$$

Lengths, masses, and distances to the respective centers of mass are measured, while corresponding inertias are identified experimentally.

TABLE I
Physical Parameters of the Setup

Parameter	First Link	Second Link
Length	$l_1=0.25\,\mathrm{m}$	$l_2=0.25\,\mathrm{m}$
Mass	$m_1=0.374\,\mathrm{kg}$	$m_2=0.232\,\mathrm{kg}$
Distance to CoM	$r_1=0.198\,\mathrm{m}$	$r_2=0.172\,\mathrm{m}$
Inertia about CoM	$J_{c1}=0.0027\,\mathrm{kg\,m^2}$	$J_{c2}=0.0023\,\mathrm{kg\,m^2}$
Gravitational constant	$g=9.81\,\mathrm{m/s^2}$	
Spring assembly	$r_1=r_4=0.045\,\mathrm{m}$, $r_2=r_3=0.03\,\mathrm{m}$ $L_0=0.055\,\mathrm{m}$	

The actuator in our setup is quite weak, with a maximum torque of $0.22\,\mathrm{Nm}$, compared to the rather big masses to be accelerated. We will clearly face performance problems for some desired motions. Therefore, a spring assembly is installed in parallel to the motor to enhance the overall actuation. However, the spring configuration must be well-tuned for a particular motion.

III. Spring Assembly

Numerous compression springs can be installed in the spring assembly as shown in Fig. 2. The torque about the first link joint that is delivered by the individual springs on the bottom $\{c_{1B},c_{2B},c_{3B},c_{4B}\}$ and on the top $\{c_{1T},c_{2T},c_{3T},c_{4T}\}$ is computed as follows

$$\tau_c(\varphi)=\begin{cases}\left.\begin{array}{l}\tau_{c_{1T}}(\varphi)+\tau_{c_{2T}}(\varphi)\\ +\tau_{c_{3B}}(\varphi)+\tau_{c_{4B}}(\varphi)\end{array}\right\} & \text{for } \varphi<0\\ \left.\begin{array}{l}-\tau_{c_{1B}}(\varphi)-\tau_{c_{2B}}(\varphi)\\ -\tau_{c_{3T}}(\varphi)-\tau_{c_{4T}}(\varphi)\end{array}\right\} & \text{for } \varphi>0\,,\end{cases} \quad (2)$$

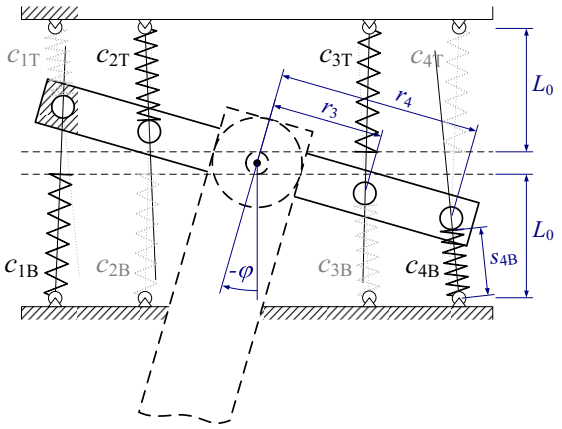

Fig. 2. Front view at the spring assembly.

where for $i=1..4$

$$\begin{aligned}&\tau_{c_{i\{B,T\}}}(\varphi)=F_{i\{B,T\}}\cos\left(|\varphi|+\arccos\left(\tfrac{L_0-\sin(|\varphi|)r_i}{s_{i\{B,T\}}}\right)\right)r_i\\ &F_{i\{B,T\}}(\varphi)=c_{i\{B,T\}}(L_0-s_{i\{B,T\}})\\ &s_{iB}(\varphi)=\sqrt{(L_0-\sin(|\varphi|)r_i)^2+(r_i(1-\cos(\varphi)))^2}\\ &\{s_{1T}=s_{4B}\,,\ s_{2T}=s_{3B}\,,\ s_{3T}=s_{2B}\,,\ s_{4T}=s_{1B}\}\,.\end{aligned}$$

In the coordinate system of the Pendubot, the angle φ is given by

$$\varphi=\pi/2+q_1\,.$$

The generated torque w.r.t. the angle φ is shown in Fig. 3 exemplified for a configuration of some standard springs [3] $c_{1B}=c_{4B}=471\,\mathrm{N/m}$ and $c_{2B}=c_{3B}=471\,\mathrm{N/m}$, respectively. Note that installing the same springs at the top of the spring assembly instead of the bottom results in the same torque function.

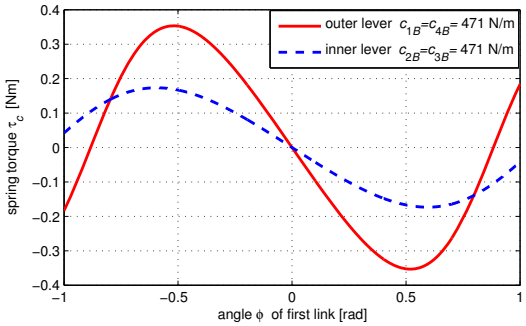

Fig. 3. Generated torque of two standard springs with a constant of 471 N/m when symmetrically installed on the inner or outer lever.

It is clear that the dynamics of our original system (1) changes by installing some springs acting on the first link. It is basically the same as introducing an additional potential torque, i.e. the gravitational torque vector changes accordingly to

$$G_c(q)=G(q)-\begin{bmatrix}\tau_c(q_1)\\ 0\end{bmatrix}. \quad (3)$$

This fact does not influence motion planning for our mechanical system, presented in the next section, but it necessarily plays some role in the feedback control action.

IV. Motion Planning

A. Concept of Virtual Holonomic Constraints

The virtual holonomic constraints approach is a generic tool for motion planning and control, especially for underactuated systems. The main idea is to reparameterize any somewhat coordinated motion as a geometric function of the generalized coordinates. If this function is preserved by some control action along solutions of the closed-loop system[1], it is called *virtual holonomic (geometric) constraint*. In particular, one has to chose a coordinate or possibly a scalar function of coordinates (for instance path length) as an independent variable θ that parameterizes the motion with respect to time. Then, the virtual holonomic constraint takes the form

$$\begin{bmatrix} q_1 \\ q_2 \\ \vdots \\ q_n \end{bmatrix} = \Phi(\theta) = \begin{bmatrix} \phi_1(\theta) \\ \phi_2(\theta) \\ \vdots \\ \phi_n(\theta) \end{bmatrix} \tag{4}$$

with $n = \dim q$. Note that the function (4) can be shaped either by observation of some real motion or by some analytical design procedure.

Suppose that there exists a control law u_* for the controlled input torques $B(q)u$ of the underactuated Euler–Lagrange system that makes the virtual holonomic constraint (4) invariant, then, the overall closed-loop system can be represented by reduced order dynamics[2] of the form

$$\alpha(\theta)\,\ddot{\theta} + \beta(\theta)\,\dot{\theta}^2 + \gamma(\theta) = 0\,. \tag{5}$$

Hence, solutions of that virtually constrained system define achievable motions of the robot with precise synchronization given by (4). It means that the whole motion is parameterized by the evolution of the chosen configuration variable θ. The smooth functions $\alpha(\theta)$, $\beta(\theta)$ and $\gamma(\theta)$ of the reduced dynamics (5) can be computed as follows from [6, Prop. 2]:

$$\begin{aligned} \alpha(\theta) &= B^\perp M\left(\Phi(\theta)\right) \Phi'(\theta) \\ \beta(\theta) &= B^\perp \Big[C\left(\Phi(\theta), \Phi'(\theta)\right) \Phi'(\theta) + M\left(\Phi(\theta)\right) \Phi''(\theta) \Big] \\ \gamma(\theta) &= B^\perp G\left(\Phi\left(\theta\right)\right) , \end{aligned}$$

where $B^\perp$ is associated with the non-actuated coordinate of the given system—in case of the Pendubot $B^\perp = \begin{bmatrix} 0 & 1 \end{bmatrix}$. Note that the reduced order dynamics (5) is always integrable, provided $\alpha(\theta) \neq 0$, which is an useful property. Specifically, the integral function

$$\begin{aligned} I(\theta, \dot\theta, \theta_0, \dot\theta_0) \;&= \dot\theta^2 - \exp\left\{ -2 \int_{\theta_0}^{\theta} \frac{\beta(\tau)}{\alpha(\tau)}\, d\tau \right\} \dot\theta_0^2 \\ &\quad + \int_{\theta_0}^{\theta} \exp\left\{ -2 \int_{s}^{\theta} \frac{\beta(\tau)}{\alpha(\tau)}\, d\tau \right\} \frac{2\,\gamma(s)}{\alpha(s)}\, ds \end{aligned} \tag{6}$$

preserves its zero value along a solution $\theta(t)$ of (5), initiated at $(\theta(0), \dot\theta(0)) = (\theta_0, \dot\theta_0)$ [7]. Note that (6) can serve as a measure of distance to a desired trajectory for the reduced system [5].

Eventually, one can also compute the nominal control input u_* required to render a desired solution $\theta = \theta_*(t)$ of (5) assuming perfectly imposed virtual holonomic constraints:

$$B(q)u = \left[M(q)\ddot{q} + C(q,\dot{q})\dot{q} + G(q) \right] \Big|_{\substack{q\,=\,\Phi(\theta) \\ \dot{q}\,=\,\Phi'(\theta)\dot{\theta} \\ \ddot{q}\,=\,\Phi''(\theta)\dot{\theta}^2 + \Phi'(\theta)\ddot{\theta}}} . \tag{7}$$

B. Periodic Motions of the Pendubot

The procedure to find periodic motions of the Pendubot is described next. The first step is to define some virtual holonomic constraint (4), e.g. polynomial function of some order. Defining a linear relation between the coordinates q_1 and q_2, and choosing q_2 as the independent parameterization variable θ gives us

$$\Phi(\theta) = \begin{bmatrix} q_1 \\ q_2 \end{bmatrix} = \begin{bmatrix} q_{10} + k(\theta - q_{20}) \\ \theta \end{bmatrix} . \tag{8}$$

For such a choice, existence of small periodic orbits of (5) around a chosen equilibrium (q_{10}, q_{20}) has been proved in [7] and is discussed in [1] for the Pendubot.

Let us focus on periodic motions about the *downward-downward equilibrium* of the Pendubot, i.e.

$$\Big(q_{10} = -\frac{\pi}{2}, \quad q_{20} = 0 \Big) . \tag{9}$$

Such type of oscillation has an apparent resemblance to a swing leg motion during human walking gaits—as an abstraction of the swinging leg, one can view the upper leg being actuated at the hip joint while the lower leg is not or at most weakly actuated by the knee. With the choice of

$$k = 0.4 \tag{10}$$

in the linear relation of the virtual holonomic constraint (8), we obtain closed trajectories for the reduced dynamics (5) around the equilibrium (9) as shown in Fig. 4a. All these periodic orbits represent achievable motions of the Pendubot with certain amplitude and period. Not all of those, however, could be easily stabilized by the present actuator. The torque required for any desired motion is simply computed by (7). The torque profiles associated to solutions of the reduced dynamics (depicted in Fig. 4a) are shown in Fig. 4b with respect to the actuated angle q_1—this representation can be advantageously used to shape the complementary actuation torques of the spring assembly.

Considering the necessary torques for achievable motions requires also a closer look at the available actuation power. In our setup there is a saturation level for the maximum torque of the motor

$$\tau_{\max} = 0.22\,\mathrm{Nm}\,,$$

i.e. not all motions depicted in Fig. 4 are feasible. Let us choose the following time periodic solution of (5) with

[1] Provided that initial conditions q_0 are chosen to satisfy the constraint.

[2] The dimension depends on the degree of underactuation; the differential equation is scalar in the case of underactuation degree one where $\dim q - \dim u = 1$.

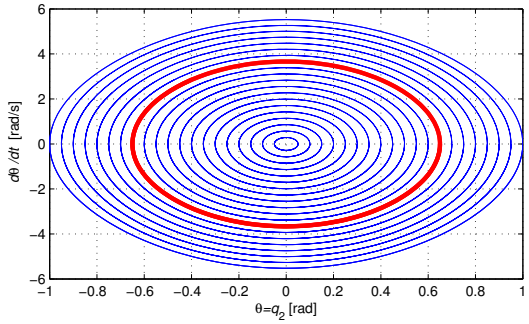

(a) Phase portrait for various solutions of the reduced dynamics.

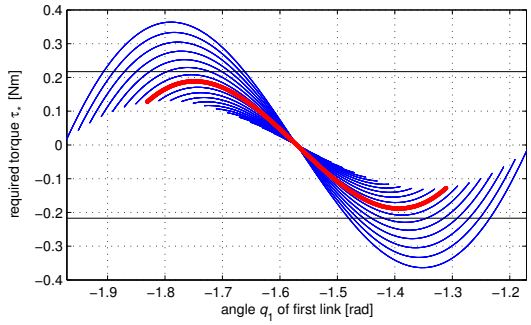

(b) Required torques w.r.t. the actuated angle q_1 for various solutions of the reduced dynamics. Saturation levels of the actuator are shown as well.

Fig. 4. Virtually constrained periodic motions of the Pendubot about the downward-downward equilibrium with $(q_{10} = -\frac{\pi}{2}, q_{20} = 0)$ and $k = 0.4$. The bold line represents the desired motion.

virtual holonomic constraints (8)–(10)

$$\theta_*(t) : \begin{cases} (\theta_*(0), \dot{\theta}_*(0)) = (0.65\,\text{rad}, 0\,\text{rad/s}) \\ T = 1.1336\,\text{s}\,. \end{cases} \tag{11}$$

that can be still performed within the available actuation power (see bold line in Fig. 4).

The main task now is to tune the passive elements of the spring assembly (see Section III) for the particular trajectory defined by (11). We aim at reducing the control effort on the original actuator by contributive spring torques.

C. Contribution of Springs to the Required Torque

A qualitative plot of torques generated by standard compression springs is already shown in Fig. 3. There are various configurations for the spring assembly and we have to select one that gives a reasonable curve close to the required torque τ_* for the desired periodic motion given by (11). Choosing some standard springs from [3]

$$c_{1B} = c_{4B} = 471\,\text{N/m} \tag{12}$$

gives such function τ_c in the interval of q_1 relevant for the motion. Since the springs become part of the control input to the first link, the motor will only have to give a reduced torque

$$\tau_{\text{red}} = \tau_* - \tau_c\,. \tag{13}$$

In Fig. 5a it can be seen that the reduced motor torque is much less than the required torque for the motion by introducing the springs as additional actuator. Looking at the absolute mechanical power (see Fig. 5b) that was used over one period it becomes even more obvious that there has been a remarkable reduction of energy expenditure to

$$P^N_{\text{red},T} = \frac{\int_{t=0}^{T} |\tau_{\text{red}}\,\dot{q}_{1*}|\,dt}{\int_{t=0}^{T} |\tau_*\,\dot{q}_{1*}|\,dt} = 26\%\,.$$

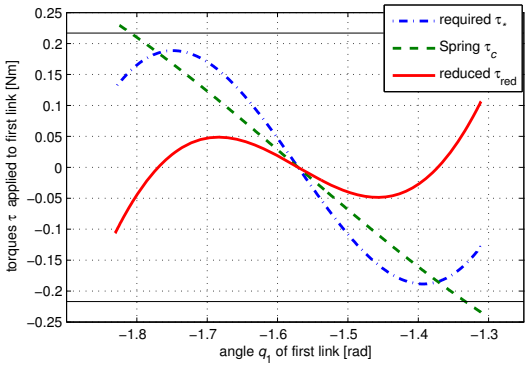

(a) Reduced torque versus originally required one w.r.t. the actuated angle q_1.

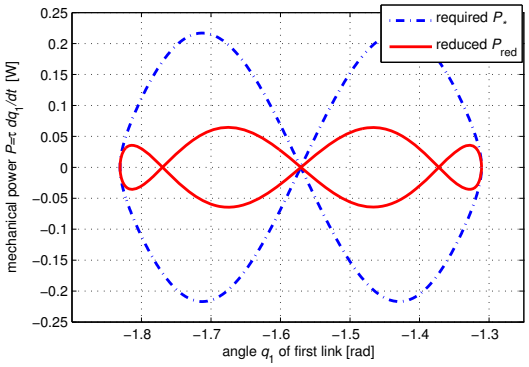

(b) Reduced mechanical power versus originally required one w.r.t. the actuated angle q_1.

Fig. 5. Reduction of torque and mechanical power for the desired motion by introducing additional spring actuators.

D. Generic Motion Planning Procedure with Subsequent Spring Selection

Let us summarize the procedure of parameterizing a particular motion and the subsequent selection of springs by the following steps:

1. Find a virtual holonomic constraint (4) for synchronization among the generalized coordinates (analytically or by observation).
2. Choose a desired trajectory of the reduced order closed-loop dynamics (5).
3. Compute the nominal torque associated to the desired trajectory (7).
4. Select or design mechanical springs that contribute to the required actuation torque.

Of course, the whole motion-planning procedure is based on the assumption that virtual constraints can be imposed on the system dynamics by a feedback control action. This will be briefly discussed in the next section.

V. Control Concept with Springs

The design step following the motion planning is the synthesis of a feedback controller with the objective to achieve contraction to the desired trajectory and to diminish effects of disturbances, uncertainties in modeling, errors in parameter estimates, etc. Here, we suggest a controller that is designed based on a transverse linearization along the desired trajectory. The derivations for the feedback control law are shown in the Appendix, where the controlled torque is given as

$$\tau_k = f(q, \dot{q}, v)\,.$$

Recall that the dynamics of the Pendubot (1) changes in terms of (3) by installing some springs acting on the first link. In fact, the torque τ_c that is generated by springs can be interpreted as mechanical feedback. It means that the controlled torque τ to the original dynamics is now composed by

$$\tau = \tau_c + \tau_k\,. \tag{14}$$

A general schematic of the control concept with springs is depicted in Fig. 6. Eventually, we expect a significant reduction of mechanical power to be delivered by the motor when the actuation is complemented by some well-tuned springs.

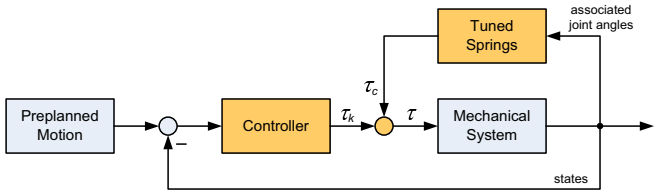

Fig. 6. Schematic of the control concept with mechanical feedback from springs.

VI. Experimental Results

The experiment is carried out with a real-time platform of the type dSPACE 1104. The angular positions q_1 and q_2 of the two links are measured by encoders with resolutions of 4096 and 3600 pulses per revolution, respectively. The angular velocities are estimated as $\hat{\dot{q}}_1$ and $\hat{\dot{q}}_2$ based on second order high-gain linear observers [2]. In order to apply the feedback control law (see Appendix) for our desired periodic motion (11), one has to find a stabilizing solution of the dynamic Riccati equation. Such $R(t)$ was found for the weighting matrices

$$Q = \mathrm{diag}(1, 1, 0.1) \quad \text{and} \quad \Gamma = 1\,.$$

Since there are frictional torques present in the real setup, one has to apply a friction compensation scheme. While there is significant friction in the first link joint, mostly induced by the motor, the friction in the second link joint is assumed to be negligible. In our case we use a a static map with estimated Coulomb and viscous properties:

$$\tau_F = F_C \mathrm{sign}(\hat{\dot{q}}_1) + F_V \hat{\dot{q}}_1\,,$$

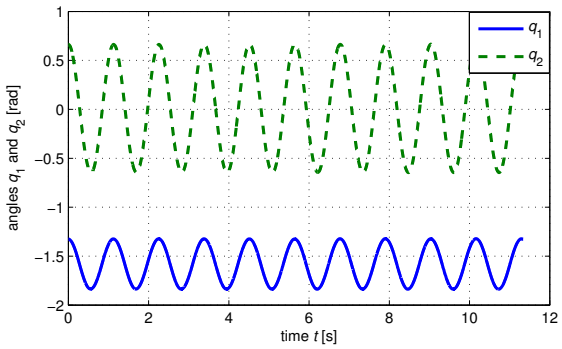

(a) Periodic oscillations in the angular positions q_1 and q_2 (for 10 periods).

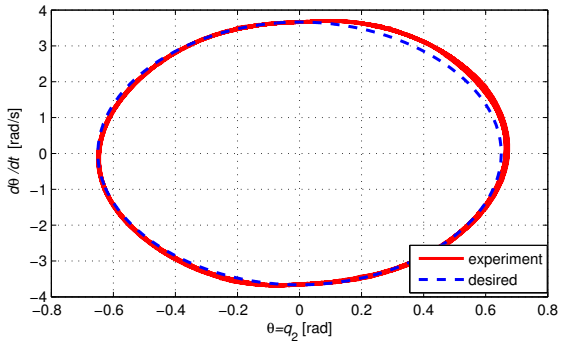

(b) Achieved phase portrait for the desired solution θ of the reduced dynamics (time span 30 s).

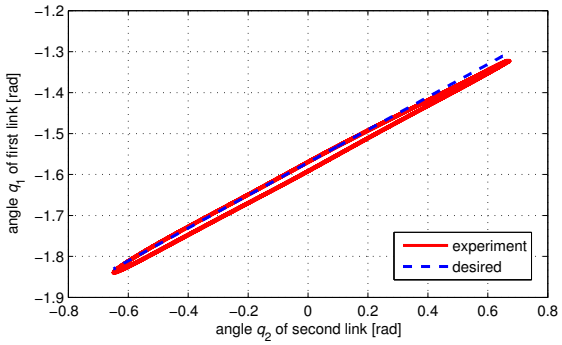

(c) Achieved virtual holonomic constraint (time span 30 s).

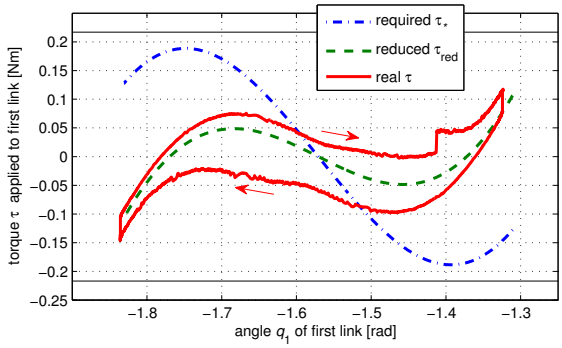

(d) Reduced motor torque with friction compensation compared to the ideally required torque for the desired motion (for one period).

Fig. 7. Experimental results of virtually constrained oscillations generated by a reduced torque from the motor utilizing the spring assembly with the standard constants $c_{1B} = c_{4B} = 471$ N/m.

where the levels of Coulomb friction are different for positive and negative velocities

$$F_C = \begin{cases} F_{Cp} & \text{for} \quad \hat{\dot{q}}_1 > 0 \\ F_{Cn} & \text{for} \quad \hat{\dot{q}}_1 < 0 \,. \end{cases}$$

The following values were identified in experiments:

$$F_{Cp} = 0.021\,\text{Nm}\,,\ F_{Cn} = 0.014\,\text{Nm}\,,\ F_V = 0.002\,\text{Nm s}\,.$$

In Fig. 7 the experimental results are shown. The controller was able to stabilize the desired virtually constrained motion (11) utilizing the springs (12) as additional actuator. The applied motor torque shows a hysteresis behavior around the ideally reduced torque which is due to the presence of friction, model uncertainties, delay, etc. However, the springs reduce the motor torque significantly. In fact, the desired motion could not even be achieved in praxi without springs because of the saturation levels of the motor.

VII. Conclusions

In this paper we demonstrated the use of mechanical springs as passive actuators in concert with a comparably weak DC motor to generate periodic motions of an underactutated planar two-link robot. The main objective of reducing the control efforts with contributive spring torques was shown. The virtual holonomic constraints approach serves as analytical tool to parameterize, plan, and stabilize desired motions. The suggested control design procedure is based on a transverse linearization along a desired trajectory. During the motion planning process one can realize a feasible range of motions within given saturation levels of the actuators. By installing a suitable configuration of springs that gives approximately the required torque for the desired motion, it is possible to reduce the control effort and consequently the power consumption of the original actuator significantly. This claim was verified in experiments for a particular periodic motion.

Appendix
Suggested Stabilizing Controller

The key procedure to derive the stabilizing controller for the Pendubot is presented below. The method is based on a transverse linearization along a desired trajectory proposed in [6], [5].

Let us introduce new independent coordinates for the Pendubot (1):

$$y = q_1 - \phi_1(\theta) \quad \text{and} \quad \theta\,,$$

where zero value of y satisfies the virtual holonomic constraints defined in (4) and (8). The first and second time derivatives of y and θ are related to the original coordinates q and their time derivatives as follows

$$\dot{q} = L(\theta, y) \begin{bmatrix} \dot{y} \\ \dot{\theta} \end{bmatrix}, \quad \ddot{q} = L(\theta, y) \begin{bmatrix} \ddot{y} \\ \ddot{\theta} \end{bmatrix} + \dot{L}(\theta, y) \begin{bmatrix} \dot{y} \\ \dot{\theta} \end{bmatrix}$$

$$\text{where} \quad L(\theta, y) = \begin{bmatrix} 1 & \phi_1'(\theta) \\ 0 & 1 \end{bmatrix}.$$

Hence, the dynamics of y can be written as

$$\ddot{y} = R(y, \theta, \dot{y}, \dot{\theta}) + N(y, \theta)\,\tau = v$$

where

$$R = [1,\ 0]\ L^{-1}\,M^{-1}(q)\,\left(-C(q,\dot{q})\dot{q} - G(q) - \dot{L}\begin{bmatrix} \dot{y} \\ \dot{\theta} \end{bmatrix}\right)\Big|_{\substack{q\,=\,\Phi(\theta) \\ \dot{q}\,=\,L\begin{bmatrix} \dot{y} \\ \dot{\theta} \end{bmatrix}}}$$

$$N = [1,\ 0]\ L^{-1} M^{-1}(q)\big|_{q=\Phi(\theta)}$$

and the feedback transformation

$$\tau = N^{-1}(y, \theta)\left[v - R(y, \theta, \dot{y}, \dot{\theta})\right] \tag{15}$$

results in a virtual control variable v.

Differentiating the integral function (6) along the trajectories of (5), one obtains dynamics transversal to solutions $\theta(t)$ [6], [5]

$$\begin{aligned} \tfrac{d}{dt} I(\cdot) &= \tfrac{2\dot{\theta}}{\alpha(\theta)}\left[g_y(\cdot)y + g_{\dot{y}}(\cdot)\dot{y} + g_v(\cdot)v - \beta(\theta) I(\cdot)\right] \\ \ddot{y} &= v\,. \end{aligned}$$

Eventually, the controller design can be based on the linearization along a desired solution $\theta_*(t)$—a linear time-variant comparison system called transverse linerarization:

$$\begin{aligned} \tfrac{d}{dt} z &= A(\theta_*(t), \dot{\theta}_*(t))z + b(\theta_*(t), \dot{\theta}_*(t))v \\ z &= [\delta I, \delta y, \delta \dot{y}]^T \end{aligned}$$

with the time-variant periodic matrix functions

$$A(\theta(t), \dot{\theta}(t)) = \begin{bmatrix} a_{11}(\theta, \dot{\theta}) & a_{12}(\theta, \dot{\theta}) & a_{13}(\theta, \dot{\theta}) \\ 0 & 1 & 0 \\ 0 & 0 & 0 \end{bmatrix}$$

$$b^T(\theta(t), \dot{\theta}(t)) = \begin{bmatrix} b_1(\theta, \dot{\theta}) & 0 & 1 \end{bmatrix}$$

$$\begin{aligned} a_{11}(\theta, \dot{\theta}) &= -\tfrac{2\dot{\theta}\beta(\theta)}{\alpha(\theta)}\,, & a_{12}(\theta, \dot{\theta}) &= \tfrac{2\dot{\theta} g_y(\theta, 0)}{\alpha(\theta)} \\ a_{13}(\theta, \dot{\theta}) &= \tfrac{2\dot{\theta} g_{\dot{y}}(\theta, \dot{\theta}, 0)}{\alpha(\theta)}\,, & b_1(\theta, \dot{\theta}) &= \tfrac{2\dot{\theta} g_v(\theta)}{\alpha(\theta)}\,. \end{aligned}$$

Exponential orbital feedback stabilization will be achieved using a solution of the continuous time-periodic dynamic Riccati equation

$$\dot{R}(t) + A(t)^T R(t) + R(t) A(t) + Q = R(t) B(t) \Gamma^{-1} B(t)^T R(t)$$

with appropriately chosen weighting matrices $Q \geq 0$ and $\Gamma > 0$. In order to use such stabilizing solution $R(t)$ for any $\theta(t)$ close to the desired trajectory $\theta_*(t)$, we have to introduce an operator $\mathcal{P}_t$, that is, projecting points of the phase plane $(\theta, \dot{\theta})$ onto a curve $\mathcal{C}_*$ defined by $(\theta_*, \dot{\theta}_*)$ of the reduced system:

$$\begin{aligned} &\mathcal{P}_t : [\theta, \dot{\theta}] \to \mathcal{C}_* \\ &\mathcal{C}_* = \left\{ [\theta_*(t), \dot{\theta}_*(t)],\ t \in [0, T] \right\}. \end{aligned}$$

Another operator

$$\mathcal{T}_* : \mathcal{C}_* \to [0, T]$$

gives the corresponding time stamp from $[0, T]$ for the point of the curve $\mathcal{C}_*$. The feedback control law

$$v(t) = -\Gamma^{-1}\, b(\theta, \dot{\theta})^T\, R\left(\mathcal{T}_*\left(\mathcal{P}_t([\theta, \dot{\theta}])\right)\right) \begin{bmatrix} I \\ y \\ \dot{y} \end{bmatrix} \tag{16}$$

guarantees convergence for the nonlinear system within a vicinity of the desired trajectory [6], [5].

References

[1] L. Freidovich, A. Robertsson, A. Shiriaev, and R. Johansson, "Periodic motions of the Pendubot via virtual holonomic constraints: Theory and experiments," *Automatica*, vol. 44, no. 3, pp. 785–791, 2008.

[2] H. Khalil, *Nonlinear systems*, 3rd ed. New Jersey: Prentice Hall, 2002.

[3] Lesjöfors Stockholms Fjäder AB, "Standard springs catalog," URL: `http://www.lesjoforsab.com`, accessed on 2008-05-26.

[4] J. Shigley and C. Mischke, *Mechanical Engineering Design*, 5th ed. Singapore: McGraw-Hill, 1989.

[5] A. Shiriaev, L. Freidovich, and I. Manchester, "Can we make a robot ballerina perform a pirouette? Orbital stabilization of periodic motions of underactuated mechanical systems," in *Proceedings of the 3rd IFAC Workshop on Periodic Control Systems*, Saint Petersburg, Russia, Aug. 29-31 2007.

[6] A. Shiriaev, J. Perram, and C. Canudas-de-Wit, "Constructive tool for orbital stabilization of underactuated nonlinear systems: Virtual constraints approach," *IEEE Transactions on Automatic Control*, vol. 50, no. 8, pp. 1164–1176, 2005.

[7] A. Shiriaev, J. Perram, A. Robertsson, and A. Sandberg, "Periodic motion planning for virtually constrained Euler–Lagrange systems," *Systems and Control Letters*, vol. 55, pp. 900–907, 2006.

[8] M. Spong and D. Block, *Pendubot user manual*, University of Illinois, Urbana-Champaign, USA, 1996.